

Torrefaction of *Pinus radiata* and *Eucalyptus globulus*: A combined experimental and modeling approach to process synthesis



Luis E. Arteaga-Pérez^{a,1}, Cristina Segura^a, Daniela Espinoza^a, Ljubisa R. Radovic^{a,b,c}, Romel Jiménez^c

^a Technological Development Unit (UDT), University of Concepción, Concepción, Chile

^b Department of Energy and Mineral Engineering, The PA State University, State College, PA 16801, USA

^c Department of Chemical Engineering, University of Concepción, Concepción, Chile

ARTICLE INFO

Article history:

Received 22 September 2014

Revised 29 May 2015

Accepted 18 August 2015

Available online xxx

Keywords:

Torrefaction

Modeling

Simulation

Aspen One v8.6

ABSTRACT

The use of wood as feedstock for the production of energy and chemicals is a strategy used by both developing and developed countries because it increases the sustainability of their energy infrastructure. Torrefaction of forest resources for co-firing and densification of biomass energy is among the most prominent alternatives. This study is focused on technical aspects of torrefaction technology by analyzing both energy and exergy changes through a comprehensive physico-chemical model (Aspen One v8.6 software) of a plant operating in mild (250 °C) and severe (280 °C) regimes. The main wood species in Chilean plantations, *Eucalyptus globulus* and *Pinus radiata*, were processed in a lab-scale apparatus to obtain the data for model calibration. We found that xylan composition in hemicelluloses has a considerable effect on global thermal efficiency, volatiles energy content, energy density, and exergy yield of torrefied product. The highest efficiency (96%) is obtained for *Eucalyptus* at 250 °C when moisture in the feedstock is ≤20%. Combustion of volatile products (torgas) for drying does not result in substantial technical benefits for the overall process; however, their post-combustion does lead to lower exergy losses.

© 2015 International Energy Initiative. Published by Elsevier Inc. All rights reserved.

Introduction

The switch from petro-economy to bio-economy has been identified as one of the most important challenges to reach sustainable development standards. Energy security concerns, excessive fossil fuel consumption, increasing pollutant emissions, and incipient climate change are the main drivers for more aggressive development of renewable energy sources. In this framework, forest biomass is the obvious candidate to replace fossil fuels, based on its abundance, renewability, and CO₂ neutrality, as well as the possibility of its conversion to higher-value-added products. Nevertheless, the barriers to be overcome toward successful development of sustainable biomass energy remain high: complex and expensive logistics associated with feedstock preparation, handling and transportation, and political, ethical, and environmental challenges of competition with agriculture for land and water (Nag, 2008; Rosillo-Calle et al., 2010). Use of woody biomass resources from forest management and forest processing industries can overcome most of these difficulties.

Regardless of the technology selected for conversion to fuels and/or chemicals, process feasibility is affected by physical, chemical, and morphological properties of biomass. High moisture content, low energy density, sensitivity to biodegradation, and hydrophilic character can

all be problems, and they should be addressed to demonstrate competitiveness with fossil fuels (Phanphanich and Mani, 2011; Agar and Wihersaari, 2012). Pretreatment methods can beneficially alter these properties by thermal, biological, or chemical means. This paper focuses on one such pretreatment, which is gaining interest because of the benefits on energy densification. Torrefaction is a thermochemical pretreatment akin to mild pyrolysis, as it occurs at relatively low temperatures, 200–300 °C, in a non-oxidizing atmosphere (Chew and Doshi, 2011; Batidzirai et al., 2013; Pighinelli et al., 2014). During such treatment woody biomass, the tenacious fiber structure of the original hydrophilic material is largely destroyed through the breakdown of hemicellulose and to a lesser degree of cellulose and lignin molecules; the solid material (biochar) becomes brittle and easy to grind (Phanphanich and Mani, 2011; Kokko et al., 2012). With the removal of light volatile fractions that contain most of the oxygen and whose utility must be considered, the material becomes more hydrophobic and its heating value increases by 5–15% at the expense of a mass loss of ~30%; former are either condensable (mainly water, organics, and lipids) or permanent gases (mainly CO and CO₂) (Bates and Ghoniem, 2012; Kiel et al., 2012; Prins et al., 2006).

The main virtues of torrefaction are its high energy efficiency, economic feasibility to replace wood pellets (Tumuluru et al., 2011; Koppejan et al., 2012; Nhuchhen et al., 2014), and its subsequent flexibility. In this sense, Harouna et al. (2015) have reported on a novel carbonization–torrefaction process to valorize cotton stalk using

E-mail address: luiseap@gmail.com (L.E. Arteaga-Pérez).

¹ Tel.: +56 41 266 1855; fax: +56 41 275 1233.

Nomenclature

C_{pd}	Heat capacity of dried wood (kJ/kg/°C).
C_{pWL}	Heat capacity of liquid water (kJ/kg/°C).
$E_{f,tot}$	Exergy flow of fuels entering the system (kW).
E_k	Exergy of stream (kW).
e_{tw}^w	Chemical exergy of torrefied wood (kJ/kg).
e_{uw}^w	Chemical exergy of untreated wood (kJ/kg).
HHV	Higher heating value (kJ/kg).
h_{wL}	Liquid enthalpy (kJ/kg).
h_{wV}	Vapour enthalpy (kJ/kg).
I_r	Irreversibilities (kW).
LHV	Lower heating value (kJ/kg).
MC_i	Moisture content (fractional).
m_{tw}	Mass flowrate of torrefied wood (kg/s).
m_{uw}	Mass flowrate of untreated wood (kg/s).
P_O and T_O	Temperature and pressure in the reference state (20 °C and 1 atm).
Q_{comb}	Heat from combustion (kW).
Q_d	Heat consumption for drying (kW).
Q_{tor}	Heat for torrefaction (kW).
T_{tor}	Torrefaction temperature (°C).
X_i	Elemental composition ($i = \%C, \%H, \%O, \%N$).
$Y_{D,k}$	Exergy destruction ratio.
Y_E	Energy yield (%).
Y_{Ex}	Solids exergy yield (%).
Y_M	Mass yield (%).

Subscripts

comb	Combustion.
d	Dry basis.
daf	Dry ash-free basis.
in	Inlet.
out	Outlet.
tg	Torrefaction gases.
tw	Torrefied wood.
uw	Untreated wood (as received).
wet	Wet basis.

Greek letters

η_c	Combustion efficiency (%).
η_d	Energy efficiency in dryer (%).
η_t	Heat transfer efficiency in the torrefaction reactor (%).

a metal kiln; they found that torrefied stalk is quite appropriate for gasification, due to the elimination of primary tars during torrefaction. This results in higher quality of the producer gas, as reported by Fisher et al. (2012) and Prins et al. (2006).

Batidzirai et al. (2013) studied the technical and economic aspects of torrefaction and provided state-of-the-art insights into its commercial potential. In particular, they discussed the thermal efficiency and mass yield of compact moving bed reactors and quantified them using mass and energy balances.

These and other authors also identified knowledge lagoons about key process phenomena especially at the plant level. Indeed, most of prior research has been focused on reaction kinetics and mechanisms, and there are few reports on the overall energy demand and process modeling.

Basic pyrolysis kinetics are commonly applied for mathematical modeling of the torrefaction process as well (Repellin et al., 2010; Sarvaramini et al., 2013). Considering the temperature range of 200–300 °C, the main processes are moisture evolution, hemicellulose decomposition, and limited degradation of lignin and cellulose. Several studies described these phenomena by considering that biomass is

converted to volatiles and biochar in a single reaction step (Repellin et al., 2010). The kinetic models of Shafizadeh and Chin and Broido-Shafizadeh have described the torrefaction of briquettes and large biomass particles (Felfli et al., 2004); such models assume parallel competing pathways in the primary pyrolysis of wood leading to char, tars, and lighter volatiles. On the other hand, the Di Blasi-Lanzetta model includes weight loss kinetics of woody biomass, as well as an intermediate product that accounts for secondary devolatilization reactions. The results of these studies have been adapted to several biomass sources (Di Blasi and Lanzetta, 1997; Prins et al., 2006b; Repellin et al., 2010; Batidzirai et al., 2013). A more global description of the process and its energy requirements was presented by Granados et al. (2014), who developed an energy/exergy analysis of torrefaction for six different biomass sources (sugarcane bagasse, banana, rice husk, palm oil fibers, sawdust, and coffee residue). The process was studied in a TGA device at 250 °C for 30 min. It was found that the largest and smallest increase in the HHV of torrefied biomass were 14.5% and 5.2% for sawdust and palm oil fiber, respectively. The best results regarding exergetic efficiency were found for sugarcane bagasse, sawdust, and rice husk. When such analysis is applied at larger scale, the results are rather different and this is discussed in Section 3.

Peduzzi et al. (2014) developed a model based on ternary diagrams and focused on the evolution and energy content of gaseous and solid fractions produced during torrefaction. Their model was validated using experimental data reported by CEA Grenoble (www.cea.fr) and other relevant literature; these results were used as a reference to calculate the relative composition of gaseous products.

Joshi et al. (2014) modeled a torrefaction system by incorporating the results of externally programmed unit operation models into Cycle Tempo software (Asimptote, 2014). Because it is well known that drying is the most energy-intensive operation in the torrefaction process, it is not surprising that these authors found that lower torrefaction temperatures result in a higher system efficiency, with improved calorific values of the torrefied solid. However, a validation of such a model was not presented and the drying process simulation did not take into account the often abundant chemically bound water in the biomass.

Syu and Chiueh (2012) carried out process simulation for biochar production from rice husk using Aspen Plus software. They reported higher product yields for lower moisture levels in the feedstock. Thermal efficiency was estimated to be 85% above autothermal operation level, which can be achieved only for moisture contents below 12%. In this simulation, volatiles exiting the torrefaction reactor were burnt in a post-combustor, and the flue gases were used for drying.

The literature summarized above highlights a dearth of plant-scale models, which would allow an evaluation of the effects of operational parameters on system efficiency indicators and thus provide more reliable tools for predicting process sustainability.

Here we aim to develop a mathematical description of the torrefaction process and simulate the behavior of two Chilean wood species: hardwood (*E. globulus*) and softwood (*P. radiata*). Experimental data obtained at the Technological Development Unit of the University of Concepción (Chile) are used for model validation. The overall thermal efficiency concept is used to quantify the effect of drying within the energy balance and to include the use of volatiles as an internal energy source. Moreover, the exergy concept is used to quantify the irreversibility in the reaction stage as well as the exergy yield (fraction of useful energy retained by solid); such indicators can be easily related to further sustainability estimations.

Materials and methods

Biomass samples

Two species (eucalyptus and pine) were selected from a 20- to 30-year-old wood plantation, located in the BioBio Region of Chile. These species were chosen for their importance in the Chilean forest industry and in the domestic and renewable energy market. Chile is one of the

nations with highest potential to develop a bioforest refinery in Latin America. The main species in Chilean wood plantations are indeed *Pinus radiata* and *Eucalyptus globulus* (>90%), with an average annual yield that exceeds 35 m³/ha (Berg et al., 2013).

The samples were characterized before and after torrefaction, using standard practice for proximate analysis of coal and coke (D3172. Standard Practice for Proximate Analysis of Coal, 2013) and elemental analysis according to ABNT-NBR-8112 in a Leco True Spec. Calorific values were determined in a Parr 6400 automated calorimeter according to the ASTM D5865-13 (D5865-13 A. Standard Test Method for Gross Calorific Value of Coal, 2013). Results for both samples are summarized in Table 1.

In addition, the thermal decomposition and volatiles evolution of both pine and eucalyptus were analyzed using TGA/GCMS. Weight loss as function of temperature was recorded in a thermobalance (Netzsch, model STA 409 PC) from 20 °C to 600 °C at 10 °C/min under nitrogen atmosphere (70 mL/min). Volatiles composition at the outlet of the thermobalance was recorded by a mass spectrometer (QMS 403C Aëolos, Netzsch) by following the evolution of principal products [2 (H₂), 18 (H₂O), 28 (CO), 32 (CH₃OH), 44 (CO₂), 46 (CH₂O₂), 60 (C₂H₄O₂), 96 (C₅H₄O₂)].

Experimental setup

The experimental system (See Fig. 1) consists of a custom-built reactor placed within three heating zone electric oven (3.2 kW). The setup is also equipped with a gas-preheating system (first zone), a high-temperature filter (0.174 m in length and 0.026 m in diameter) equipped with a heating jacket and a K-type thermocouple, a water-cooled condenser coupled to a cooling bath to control the temperature at 4 °C, and an electrostatic precipitator (operating voltage: 15 kV). The reactor is a 0.54 m long stainless steel (316S) device with an inner diameter of 0.0508 m. It is operated vertically and is equipped with an internal support (frit with perforations of 0.001 m) where the biomass sample is placed. The temperature profile inside the reactor is monitored at three points, using a set of K-type thermocouples: at the bottom, in the biomass bed, and at the exit of the reactor. Heat transfer for torrefaction is favored by a constant flow of preheated nitrogen (2 L/min), at the bottom of the oven. All the lines and equipment within the experimental setup are well insulated. Two sets of experimental conditions were studied: residence times of 15 and 30 min, and temperatures of 250 and 280 °C for two-category variables (eucalyptus and pine) corresponding to a 2² factorial design. All the experiments were carried out at 10 °C/min, and residence time was computed once the reaction temperature was reached (see temperature profile in Fig. 1). After each run, the nitrogen flow was interrupted, and the reactor was rapidly cooled by an external flow of air. Experiments were carried out using 10 g of biomass (previously

sieved to 2–4 mm size); particle sizes were selected to reduce the transport resistances, as reported in (Bates and Ghoniem, 2013).

The torrefied samples were characterized using the same methods described above. The main measures of merit were mass and energy yield, with special attention paid to the latter because the fraction of energy retained by the solid after treatment is important for its potential use in co-firing or combustion applications:

$$Y_M(\%) = 100 * (m_{tw}/m_{uw})_{daf} \quad (1)$$

$$Y_E(\%) = Y_M * (HHV_{tw}/HHV_{uw})_{daf} \quad (2)$$

Furthermore, the H/C and O/C ratios of torrefied wood were conveniently represented in a van Krevelen diagram to clarify its relationship to the composition of other solid products.

Plant simulation

The comprehensive torrefaction model developed in this section is implemented in the Aspen One v8.6 simulation software. The experimental data were used to validate the model for both wood samples.

Process description

The process flow diagram (PFD) of Kiel et al. (2012) is a convenient point of departure. As shown in Fig. 2, it was used to develop the PFD for the base case. It involves four stages: drying (moisture reduction), torrefaction (chemical reaction), combustion (energy production), and cooling of torrefied products (product conditioning).

The feedstock consists of uniformly sized wood chips containing 20–50% water. The moisture content should be reduced to 5–10% prior to torrefaction, to avoid incomplete combustion of wet torrefaction gases and minimize the process residence time, as reported by Koppejan et al. 2012. The torgas and an extra wood inlet are used in the combustion stage to fulfill the energy requirements of both drying and torrefaction. During torrefaction, the water still contained in the wood structure (superficial or chemically bound) is driven out together with some lights organics (e.g. sugars, polysugars, alcohols, furans, ketones, and lipids) which, in addition to the torrefied solid, are the main products. Torrefied wood is then cooled to below 50 °C, to reduce the risks of spontaneous ignition. It is then slowly exposed to ambient air (oxygen and moisture) in order to minimize its reactivity.

Two alternative process simulations (dashed lines in Fig. 2: Alt 1. and Alt. 2) were studied:

Alternative 1. Torgas exiting the reactor is fed directly to the external combustor to supply the heat required by reaction and drying stages (this is the basic process of Kiel et al. (2012)).

Alternative 2. Torgas is used for drying and subsequently it is burned in the combustor to supply the heat required by torrefaction.

Model formulation

Fig. 3 summarizes the torrefaction model. It is divided into sub-units that simulate drying, torrefaction, combustion, and product conditioning. In addition to the Aspen One modules, we used custom models to estimate the composition of volatiles and the extra feedstock needs for satisfying the energy balance.

The following key assumptions are used: (i) all calculations are in steady state; (ii) the Redlich–Kwong–Soave (RKS) equation of state was used for property estimation; (iii) untreated and torrefied wood were defined using proximate and ultimate analyses data and they were treated as unconventional solids; (iv) air composition is assumed 79% nitrogen and 21% oxygen on molar basis; (v) the model is independent of particle size and intra-particle heat, and mass transfer is neglected.

Table 1
Characterization of untreated biomass.

	Proximate analysis		Ultimate analysis		
	Pine	Eucalyptus	Pine	Eucalyptus	
Moisture (%)	6.82	7.12	Carbon (%)	48.94	48.72
Volatiles (%)	77.71	76.50	Hydrogen (%)	6.91	6.70
Fixed carbon (%)	15.17	16.20	Nitrogen (%)	0.12	0.02
Ash (%)	0.30	0.18	Sulphur (%)	0	0
HHV (MJ/kg)	18.89	17.45	Oxygen (%) ¹	44.03	44.56
Chemical composition	Experimental²		Atomic balance		
Cellulose (%)	44.5	51	44.19	51.1	
Hemicellulose (%)	28.5	26	28.8	26.7	
Lignin (%)	27.7	23	27.0	22.2	

¹ Oxygen is calculated by difference from C, H, N, considering the low ash content.

² The procedure used to determine the chemical composition by atomic balance was reported by (Burhenne et al., 2013). Lignin composition was taken from (Esteves Costa et al., 2014).

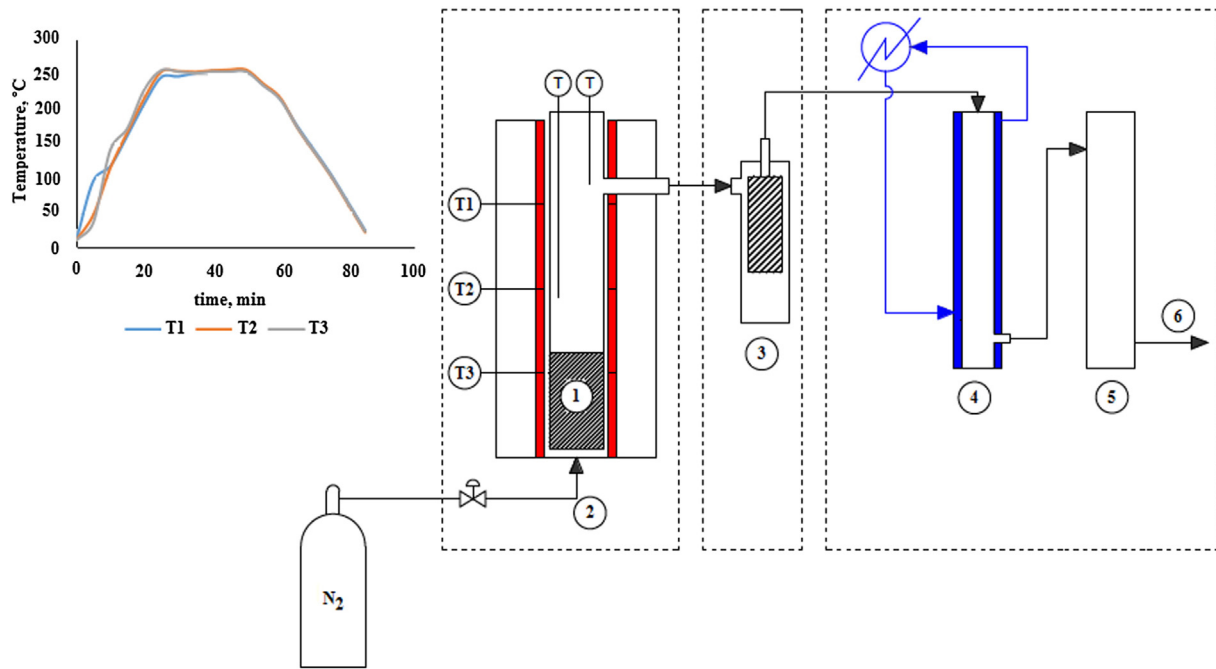


Fig. 1. Experimental setup. Torrefaction facility at the UDT. (1) Nitrogen preheater, (2) reactor, (3) high-temperature filter, (4) condenser coupled to a cooling bath, (5) electrostatic precipitator, (6) gas sampling point.

Drying

This is the most energy-intensive stage in torrefaction and it is simulated as a continuous single-stage (double-contact) dryer (Gassner and Maréchal, 2009; Basu, 2013; Batidzirai et al., 2013). According to Amos (1998) and Holmberg and Ahtila (2005), there are several designs (rotary, flash, discs, cascade) and schemes (direct contact, indirect contact, with heat recovery) to perform the drying of biomass. The selection of a specific design depends mainly on moisture content, particle size, and drying medium (air, exhaust flue gas, or superheated steam). The most common way to evaluate the efficiency of a drying process is by calculating its specific heat consumption (amount of heat supplied per kg of moisture removed) (Holmberg and Ahtila, 2005).

Here, the energy balance is solved by assuming that untreated wood enters at atmospheric conditions and its moisture content is gradually reduced to 10%. Flue gas from combustion stage (Alt. 1) or torgas (Alt. 2) is used as heating medium. The drying process was simulated using

two unit operation blocks; a stoichiometric reactor (DR-01), and a flash separator (DR-02). Although wood drying is not normally considered a chemical reaction (even though some chemically bound water may be released), this approximation allows the model to convert a fraction of unconventional component (moisture in wood) to conventional water and to calculate the heat needed to vaporize this water. A Fortran block is used to solve the mass balance in the process. The heat needed in this stage is included in the system balance as a heat sink and the value was compared to that estimated by Eq. 3 from Basu (2013) and Zakri et al. (2013).

$$Q_d = \frac{m_{uw}}{\eta_d} \left\{ \frac{(MC_{wet} - MC_d) \times (h_{wL} - h_{wV}) + [(1 - MC_{wet}) \times Cp_d + MC_d Cp_{wL}](T_{out} - T_{in})}{\eta_d} \right\} \quad (3)$$

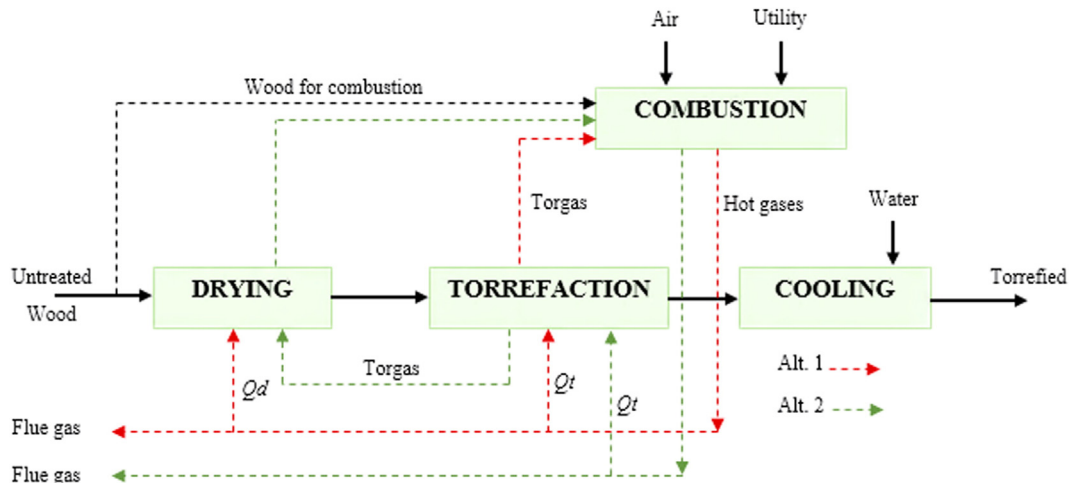


Fig. 2. Overview of the process flow diagram.

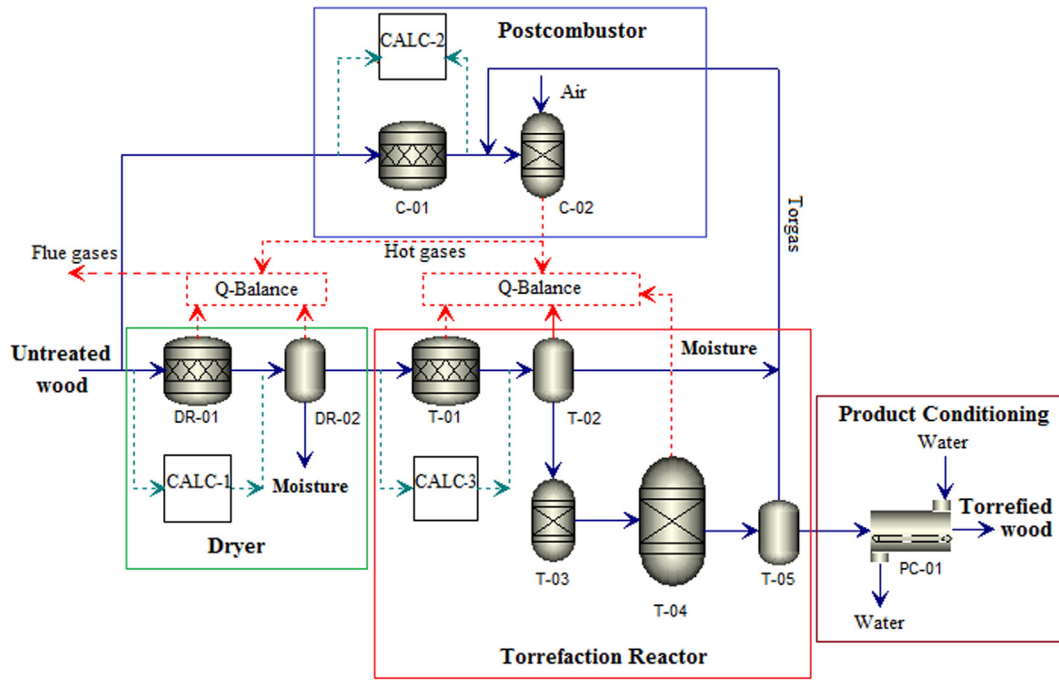


Fig. 3. Flow diagram of the model.

Dryer efficiency (η_d) was assumed to be 75% (Holmberg and Ahtila, 2005; Koppejan et al., 2012).

Cooling

The torrefied wood cooler is a water-cooled screw conveyor. This heat exchanger is calculated by a HeatX block (PC-01), considering solid and liquid phases. Cooling water utility is calculated by considering a 55 °C rise in ambient temperature. Negligible pressure drop and frictional heat losses are assumed for this stage.

Combustion

As described in Section 3.1, this stage is included to balance the energy requirements in the system. Two different fuels were considered: *torgas*, and a fraction of wood. The Gibbs free energy minimization method is used to model their combustion (C-02). Since the Gibbs free energy of wood cannot be calculated precisely (because it is a unconventional component), an extra yield reactor (C-01) and a calculator block are included to convert non-conventional wood constituents into their conventional homologues prior to combustion module calculations. Energy content of *torgas* is estimated using the HHV of individual constituents ($x_i \cdot HHV_i$ in MJ/kg). The potential for autothermal operation is determined based on this parameter. A set of possible combustion products is specified (CO, CO₂, H₂O, C, and ash) to determine the composition of combustion gases. The needs of extra wood to balance the energy requirement for drying and torrefaction are calculated by minimizing the objective function represented in Eq. 4 using the Secant method:

$$\text{MIN} = \left[(Q_{\text{comb}})^2 - (1/\eta_c * (Q_d + Q_{\text{tor}}))^2 \right] \quad (4)$$

Q_i are the heat sinks/sources (*comb* = combustor, *d* = dryer, *tor* = reactor) in kW.

One of the most important operational complications is the management of the heating media. According to Koppejan et al. (2012), there are several ways to fulfill the heat needs in a torrefaction system: (i) a fraction of the torrefaction gas is preheated with flue gas and fed into the reactor, with the drawback that volatiles can react and form tars

via repolymerization; (ii) the volatiles can be burned downstream of the torrefaction unit and flue gases recycled into the reactor, this has the advantage of efficient heat transfer to biomass particles but can reduce the mass yield due to the oxygen present in the flue gas; an alternative is the indirect heating using flue gas whose main drawback is the lower thermal efficiency; (iii) recirculation of (supercritical) steam for direct or indirect process heat (this alternative needs a boiler which may be fueled with torrefaction gas or biomass). Here we assumed direct heating with flue gas. Its temperature and flowrate were controlled in the combustion stage so as to provide a specific heat flow defined in Eq. 4.

Torrefaction

An arguably novel concept for modeling this stage is presented here. Torrefaction is considered a mild pyrolysis process occurring at atmospheric pressure and 250–280 °C. The reaction stage is modeled as a set of unit operation blocks (T-01 to T-05) integrated to user-defined functions to include the phenomena described by Basu (2013) and Zakri et al. (2013), as follows.

Initial heating: In this phase, heat is merely used to raise the temperature of wood.

Pre-drying: the temperature is constant and the free water constantly evaporates from the wood until moisture in the pores reaches its critical level.

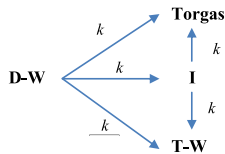
Post-drying: The physically bound moisture is released and the wood becomes essentially water-free.

Torrefaction

The dried solid is maintained at reaction temperature for predefined residence time during which depolymerization of hemicellulose, cellulose, and to a lesser extent lignin produces volatiles (gases and vapors) and solid products. The extent and mechanism of decomposition of these pseudo-components are functions of torrefaction severity (Chen and Kuo, 2011). The first three steps are described using two unit operation blocks, a stoichiometric reactor (T-01), and a flash separator

(T-02), in a similar way to that used for drying, but solving the mass balance for final moisture content being equal to that of torrefied solid.

Torrefaction itself is simulated by considering two decomposition steps: (i) fractionation of wood into its three pseudo-components (hemicellulose, cellulose, and lignin), and (ii) production of torrefied solid and volatiles. These steps are both represented using yield reactors (T-03 and T-04) and a calculator block. As torrefaction occurs between mild and severe regimes (≥ 250 °C) (van der Stelt et al., 2011), the calculation assumes hemicellulose to be the more reactive component, and only slight conversion of lignin and cellulose pseudo-components of both wood samples (Chen and Kuo, 2011). The parallel/consecutive reaction scheme proposed by Bryden et al. (2002) was used to adequately describe the mechanism of the process.



Here, D-W refers to dried wood, T-W to torrefied wood, and I is a tarry intermediate.

The anhydric weight loss (AWL) and the torrefied solid composition are calculated using experimental data (Table 2). The fraction of volatiles is calculated by a mass balance and the composition of gases is estimated using a similar procedure to that reported by Peduzzi et al. (2014). Water, acetic acid ($C_2H_4O_2$), formic acid (CH_2O_2), methanol (CH_3OH), furfural ($C_5H_4O_2$), carbon dioxide, and carbon monoxide were considered as the most abundant volatile species, based on TGA/GCMS results (Fig. 4) and on the reports of Bates and Ghoniem (2012), Kiel et al. (2012), Prins et al. (2006), and Park et al. (2015). Solid/gas phase separation is calculated by a flash block (T-05).

The torrefaction heat requirements result from the energy balance of all the stages described here, and they are compared to values calculated using Eq. 5 (Zakri et al., 2013).

$$Q_{tor} = \frac{m_{dw}}{\tau_{tor}} \{ MC_d (h_{wL} - h_{wV}) + (1 - MC_{wet}) Cp_d (T_{out} - T_{in}) \} \quad (5)$$

Table 2 contains a summary and a detailed description of each module.

Table 2
Description of models.

Stage	Aspen blocks/ID	Description
Drying	RStoic/DR-01	Stoichiometric reactor model and flash separator are combined to simulate drying (see text). Solves the mass balance by relating conversion to moisture removal.
	Flash2/DR-02 Calculator-1	
Combustion	RYield/C-01	Converts non-conventional constituents in the wood into their homologues. A calculator block is integrated to specify the yields. Minimization of Gibbs free energy for specific reactants/products.
	RGibbs/C-02	
	Calculator-2	
Torrefaction	RStoic/T-01	Stoichiometric reactor model and flash separator simulate drying stage as for drying. RYield models are used to split wood into cellulose, hemicellulose, and lignin and to specify product distribution for volatiles and torrefied wood. Flash2 calculates separation of solid and volatile phases at reactor conditions.
	Flash2/T-02	
	RYield/T-03, T-04	
	Flash2/T-05	
Product conditioning	HeatX/PC-01	Simulates heat exchange between torrefied wood and water considering a countercurrent arrangement and negligible heat and pressure losses.

Measures of merit

The main measures of merit in torrefaction are the change in energy content of the solid and the mass lost during wood processing (Eq. (1) and Eq. (2)). Here we present a broader discussion by including energy and exergy balances.

Energy

The definitions adopted by Bates and Ghoniem (2013) are included to study the process performance as a function of feedstock nature, torrefaction temperature, and moisture content of untreated wood. Accordingly, thermal efficiency is the ratio between net energy flow produced in the torrefaction plant and the energy consumed during conversion (fuel entering the system). Net energy (numerator in Eq. (6)) results from the difference between its total flow leaving the system in products streams and the heat consumed in drying (Q_d) and torrefaction (Q_{tor}) stages.

$$\eta (\%) = 100 \times \frac{[(m_{tw} * HHV_{tw} + m_{tg} * HHV_{tg}) - (Q_d + Q_{tor})]}{m_{uw} * HHV_{uw}} \quad (6)$$

The ratio of the heat required for drying to the total process heating needs (Q_d/Q_t) is used to clarify the effect of initial moisture on the heat balance.

The HHV of the volatiles is calculated from individual constituent contributions using the data reported by Bates and Ghoniem (2013); alternatively, the correlations presented by Channiwalla and Parikh (2002) can be used. The HHV for solids was measured; once the model was implemented in Aspen One, calculations of this parameter were made based on the elemental composition of streams, using correlations reported by Uemura et al. (2010) and Channiwalla and Parikh (2002).

Exergy

Exergy is used here in its conventional sense as the maximum work that can be produced when a heat or a material stream is brought to equilibrium with respect to a reference environment. Here the reference state is $T_0 = 20$ °C, $P_0 = 1.0$ atm and contains 75.67 %v/v N_2 , 20.35 % of O_2 , 0.03 % of CO_2 , 3.03 % of H_2O , and 0.92 % of Ar (Kotas, 1995). The exergy analysis is focused on solids by including a new concept to assess torrefaction efficiency, *exergy yield*:

$$Y_{Ex}(\%) = Y_M * (e^w_{tw}/e^w_{uw})_{daf}$$

This quantity allows to estimate the effect of torrefaction on the exergy content of biomass and hence is a measure of the useful energy retained by the solid after treatment.

The exergy of pine and eucalyptus is calculated from the statistical correlations of (Szargut and Styrylska, 1964).

$$e_i^w = \beta \times LHV_w \quad (7)$$

$$\beta = \frac{1.044 + 0.016 \left(\frac{x_H}{x_C} \right) - 0.349 \left(\frac{x_O}{x_C} \right) \left[1 - 0.53 \left(\frac{x_H}{x_C} \right) + 0.049 \left(\frac{x_N}{x_O} \right) \right]}{1 - 0.412 \left(\frac{x_O}{x_C} \right)} \quad (8)$$

Moreover, the main irreversibility and the exergy destruction coefficient for reaction stage are calculated by solving the exergy balance (Eq. 9):

$$\sum E_{in} = \sum E_k + I_r \quad (9)$$

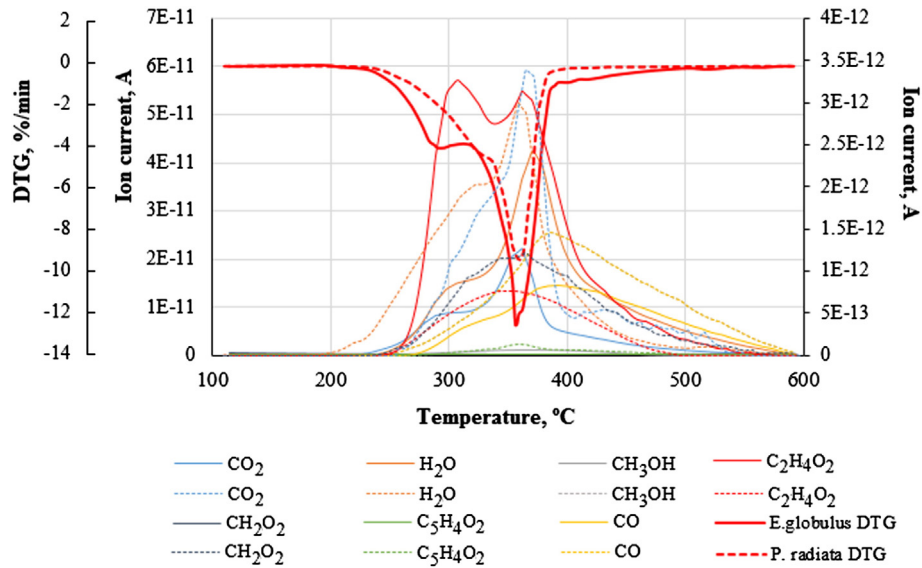


Fig. 4. Results of TGA/GCMS. Volatile species evolution for pine and eucalyptus.

Exergy destruction by irreversibility and losses in torrefaction assumes the influence of physical and chemical exergy of the streams and the exergy of heat (Carnot parameter):

$$I_r = \sum_{i=1}^n e^{ph+ch} - \sum_{i=1}^m e^{ph+ch} + \left(1 - T_o / T_{tor}\right) Q_{tor} \quad (10)$$

With: $i = \text{inlets}, j = \text{outlets}$.

The exergy destruction ratio (Eq. 11) is defined as the ratio between the irreversibilities associated to the torrefaction I_r and the total exergy of fuel entering the system $E_{f,tot}$.

$$Y_{D,k} = I_r / E_{f,tot} \quad (11)$$

Here, $E_{f,tot}$ includes the exergy of biomass and air entering the reactor and heat recovery system.

Results and discussion

Thermal decomposition and volatiles evolution.

The differential thermograms (Fig. 4) reveal that during decomposition of both pine (dashed lines) and eucalyptus, two different peaks and, therefore, two degradation processes, corresponding to hemicellulose and cellulose, were observed. The first occurs at 293 °C for eucalyptus and 330 °C for pine. The shift between them is attributed to hemicellulose in these woods (hard and soft, respectively). This effect also may lead to differences in the mass yields during torrefaction, as discussed by Basu (2013). The second peak (358 °C for eucalyptus and 360 °C for pine) characterizes the maximum decomposition rate of cellulose. The case of lignin is more complex, since it can decompose in the entire temperature range Basu (2013).

The corresponding GC/MS results are presented in Fig. 4. As expected, there is a strong signal of carboxylic acids (acetic and formic), H_2O , CO_2 , and CO in the active torrefaction stage, which is evidence of biomass dehydration and decarboxylation (Tumuluru et al., 2011; Chen et al., 2015a). All signals were normalized (by weight and heating rate), hence they are a good qualitative measure of the volatiles composition. The compounds detected at 250–300 °C are used in the modeling stage phase of this study.

Experimental torrefaction

Representative results of torrefaction experiments are summarized in Table 3. The mass and energy yields, HHV, and elemental composition were the main parameters used to characterize the processing of both wood samples.

Changes in principal element content (C, H, O) are in very good agreement with those reported by van der Stelt et al. (2011), and this lends additional support to the calculations reported below. Mass yield is a common indicator of torrefaction effectiveness, and in combination with the HHV value of products, it provides a measure of the energy retained by the solid (energy yield). Mass yields of both *E. globulus* and *P. radiata* varied between 56% and 85% at all the conditions explored, being consistently lower for the former by 4–12%. Hemicellulose in eucalyptus (hardwood) is basically formed by glucuronoxylans. According to Chen et al. (2015), xylan content in eucalyptus varies between 11 and 22 wt%, while for pine, being a softwood, galactoglucomannan only reaches 6–10%, as experimentally determined by Reyes et al. (2013). Xylans are the most reactive components within the torrefaction temperature range, and hence they degrade faster than any other solid wood component (Prins et al., 2006b; Basu, 2013); therefore, even when both pine and eucalyptus have similar hemicellulose contents (Table 1), the mass yield is rather different. Other evidence of this fact is the ratio between mass and energy yields. At 30 min and 250 °C, the mass/energy yield for pine is 0.94 while for eucalyptus it is 0.83; this is due to the fact that hardwood produces mainly water and acetic acid during torrefaction, and hence the energy loss is low compared to that of softwood, resulting in higher energy density of the solid. Furthermore, elemental analysis of the raw material and the torrefied products confirms

Table 3
Results of experimental torrefaction tests.

Parameters	Pine		Eucalyptus	
Time (min)	15	30	15	30
Temperature (°C)	250	280	250	280
C, %	51.37	52.86	52.05	53.66
H, %	6.74	6.52	6.38	6.33
N, %	0.14	0.19	0.16	0.041
O, %	40.23	40.05	41.07	39.54
Y_M (%) _{daf}	85	68	84	65
Y_E (%) _{daf}	87.29	73.07	89.64	70.88
HHV _{daf} (MJ/kg)	19.4	20.3	20.16	20.6
			19.5	20.9
			19.6	21.0

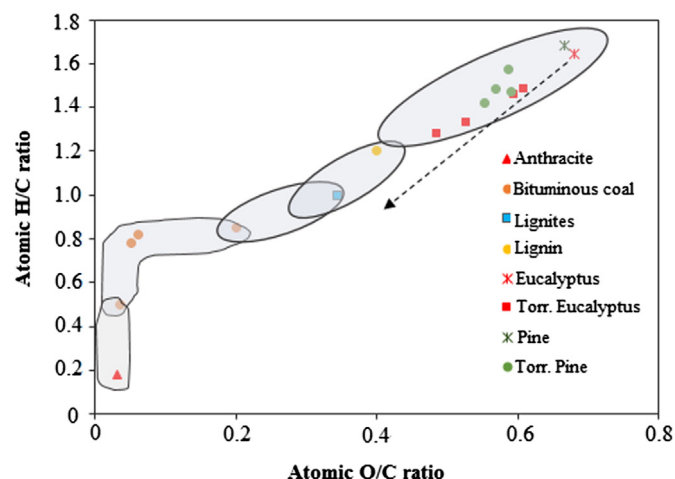


Fig. 5. van Krevelen representation of biomass (pine and eucalyptus) and torrefied biomass.

that the influence of temperature on carbon content is more important than that of time. Chew and Doshi (2011) reported similar results under the same conditions. The structure of hemicellulose and the rupture of oxygen functional groups are responsible for the increase in carbon content. Untreated pine/eucalyptus had O/C ratios of 0.67/0.68 and H/C ratios of 1.68/1.64, and after torrefaction at 280 °C and 30 min, both were reduced to minimum values of 0.48/0.55 and 1.28/1.42, respectively. This is a very desirable result because, as it is represented in a van Krevelen diagram (Fig. 5), the composition of both wood samples moves toward the fossil fuels region, thus becoming a potential replacement fuel for co-firing in conventional boilers; indeed, this may be among the most promising applications for torrefaction.

The maximum energy yields for eucalyptus (88.7%) and pine (89.6%) were found at the same operating conditions (250 °C and 30 min). Energy yield based upon mass yield can be viewed as an indicator of energy lost during torrefaction; according to Chew and Doshi (2011), it varies between 55% and 95% for woody biomass, and this is indeed the case in the present study. Results obtained here are also in good agreement with those reported by Chew and Doshi (2011), Almeida et al. (2010), and Basu (2013) for similar wood species.

It can be inferred therefore that operation at 30 min residence time produced the best performance indicators, and hence this condition will be used to simulate the process at a larger scale.

Table 4
Model results for *E. globulus* and *P. radiata*. Initial moisture (30%).

Parameter	Pine			Eucalyptus		
	250 °C	280 °C	StDv 250/280 ¹	250 °C	280 °C	StDv* 250/280
Mass yield (Y_M), %	83.1	65.1	0.63/0.07	80.1	59.2	0.77/2.2
Energy yield (Y_E), %	89.2	71.3	0.31/0.30	90.7	72.1	1.4/1.47
HHV _{tw} (MJ/kg) ²	20.2	20.7	0.027/0.26	19.8	21.5	0.13/0.33
<i>Volatiles weight composition (model predicted)</i>						
H ₂ O, %	53	49.1		57.1	50.2	
C ₂ H ₄ O ₂ , %	2.8	3.6		6.49	11.4	
CH ₂ O ₂ , %	9.3	11.7		1.96	2.8	
C ₅ H ₄ O ₂ , %	0.21	0.3		0.71	0.3	
CO ₂ , %	9.4	10.6		9.62	10.3	
CO, %	5.31	8.7		7.57	7.7	
CH ₃ OH, %	1.53	2.01		1.51	1.3	
H ₂ , %	0	0.001		0.0	0.0	
Other	16.45	13.98		15.04	15.9	
HHV _{tg} (MJ/kg)	5.52	5.70		5.69	8.45	

¹ StDv (Standard deviation) are calculated in reference to values in Table 3.

² The fraction of HHV corresponding to tars was calculated using the fraction "others" and an average of the HHV of heavier compounds detected by TGA/GCMS (see Fig. 4).

Model calibration

The results from experimental runs for eucalyptus and pine were used to assess the performance of the model. Table 4 summarizes the analyses for both temperatures (250 and 280 °C) at 30 min residence time. The variables used for comparison are the mass and energy yields, HHV of torrefied biomass and torgas (volatiles), and the total process heat demand. These parameters were selected based on their importance in characterizing the system energy performance and combustion properties of torrefied wood. The standard deviation (StDv) is used as a measure of model accuracy as well as the relative difference between observed (Table 3) and calculated values (Table 4).

From Table 4, it can be concluded that model results are in good agreement with experimental data. The heat balance of the process is a nonlinear function of weight loss and of change in the elemental composition of untreated and torrefied wood; hence statistical differences between mass and energy yields influence the global heat consumption estimates. Discrepancies between all measured and calculated mass and energy yields are considered negligible, with an average relative difference below 3% for pine and 2% for eucalyptus; considering that these parameters are complex functions of conservation equations in the dryer and reactor, as well as of torrefaction kinetics, this is a satisfactory result. The heat requirement for drying and torrefaction was compared to the calculated one (Eq. 3 and Eq. 5) and to those of Basu (2013): less than 2% relative discrepancy was found. The energy content of volatiles varied between 5.5 and 8.45 MJ/kg_(db) for both wood samples; these values are within the range (4.4–16 MJ/kg), reported by Park et al. (2015) and Bates and Ghoniem (2013). A very interesting result is a gap in the HHV_{tg} difference between eucalyptus and pine (especially at 280 °C): during torrefaction, hardwood releases mainly acetic acid and water, while softwood releases mostly formic acid (5.55 MJ/kg) whose heating value is almost three times less than that of acetic acid (14.6 MJ/kg). The best results are thus exhibited for eucalyptus, based upon the energy densification reached and the energy content of the evolved volatiles. Hence, plant simulation and synthesis were focused on this hardwood species.

Plant simulation and synthesis

The torrefaction model described in the preceding sections is used here to simulate various case studies. Base case conditions are presented in Table 5.

Table 6 summarizes the results of the mass and energy balances for the base case. These were solved for Alt. 1 in Fig. 2 where torgas and a fraction of biomass are burnt to supply system heat requirements.

Approximately 5.1% of the wood entering the system is spent to fulfill the energy requirements, mainly for drying, which is at about 72% of the total for this case. The volatiles exiting the reactor (torgas) are combusted together with the extra wood. Considering only the

Table 5
Conditions for the base case simulation of eucalyptus torrefaction.

General conditions	Value
System capacity, kg/h	100
Biomass inlet temperature, °C	20
Operating pressure, atm	1.0
Excess air in combustion, %	20–30
Dryer	
Moisture in/out, %	40/10
Drying agent temperature, °C	180
Torrefaction	
Temperature, °C	250
Residence time, min	30
Cooler	
Water inlet/outlet temperature difference, °C	55
Torrefied biomass outlet temperature, °C	50

Table 6
Base case mass and energy balances for torrefaction of eucalyptus.

Streams	Untreated wood	Torgas	Torrefied wood
Mass flow, kg/h	100	10.47	51.74
Temperature, °C	15	250	80
Carbon, w/w %	43.55	2.03	50.01
Moisture, w/w %	40	50.2	3.37
HHV _{daf} , MJ/kg	17.45	9.75	19.8
Total heat required, kW	41.70	–	–
Energy efficiency, η	88	–	–
Extra wood, kg/h	5.36	–	–
Cooling water, kg/h	72.8	–	–

use of torgas for heat production, 89% of the energy consumed in the reactor can be supplied and the remaining 11% should be produced with wood.

Effect of moisture

Batidzirai et al. (2013) demonstrated that biomass nature influences the mass and energy balances of the torrefaction processes. Among the operating variables, feedstock moisture and torrefaction temperature are the most relevant parameters in the energy balance; both are used here to evaluate system performance. Considering the results reported in the previous sections, only eucalyptus is considered for such simulation. The measures of merit are energy efficiency, feed/product ratio (F/P), and the fraction of heat used for drying. All the calculations are for Alt. 1 in Fig. 2. Fig. 6 shows the trends in both thermal efficiency (Eq. 6) and F/P ratio with moisture content.

Below 20% pre-drying is not necessary and the process scheme changes; on the other hand, above 50% air drying of biomass before processing will usually be required. Thermal efficiency is seen to decrease with increasing moisture content, as expected: there is a need for extra wood (see trend in the F/P curves) in the feedstock, to satisfy the process energy requirements, especially for drying (See also Fig. 7 below). From Eq. 5, a 45–33% increment is estimated in the extra fuel requirement for 30% variation in the moisture content with the corresponding penalty to the total energy efficiency. The F/P results are within the theoretical range of 1.35–3.6 reported by Batidzirai et al. (2013).

Fig. 7 shows how Q_d/Q_t increases with moisture content, an effect that was mentioned by Basu (2013) and is independent of torrefaction temperature when pre-drying is carried out externally. These results indicate that most of the research efforts should focus on drying, for

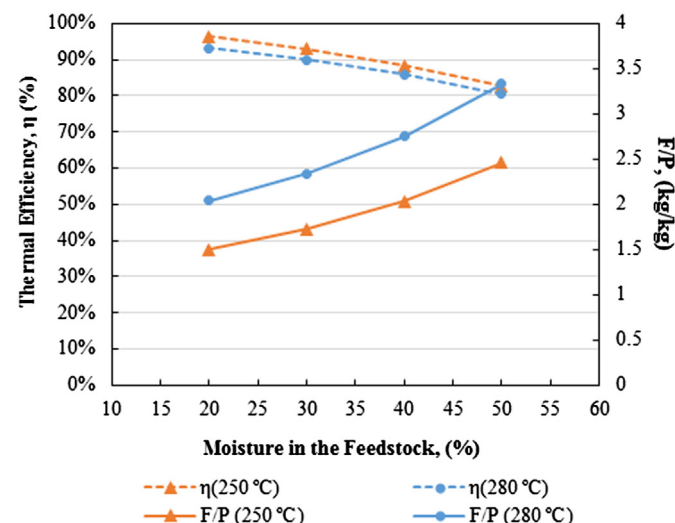


Fig. 6. Effect of feedstock water content on thermal efficiency. 250 < T < 280 °C.

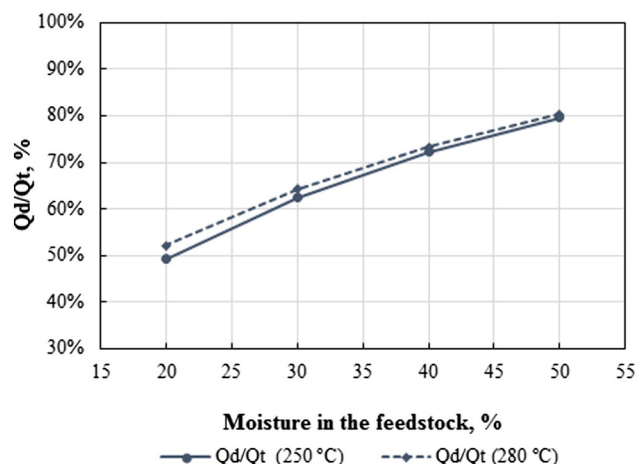


Fig. 7. Effect of water content on the heat balance. T = 250–280 °C.

which, even at moisture contents as low as 20%, the Q_d/Q_t ratio is as high as 50%. It should be noted that the results in Fig. 6 and Fig. 7 derive from the description of the drying stages reported in Section 3.2.

An interesting result is obtained when thermal efficiency and F/P ratio are compared (see Fig. 6). It is reasonable to assume a linear relationship between them. Nevertheless, even when F/P is higher at 280 °C so is the efficiency, due to a reduction of extra wood requirements. This is due to the fact that mass yield is lower at 280 °C than at 250 °C (see Tables 3 and 4) and also to the higher energy content of the volatiles (at about 16% of energy yield in gas), which results in a compensation effect. Peduzzi et al. (2014) reported similar behavior, but their argument is based on the concept of autothermal operation, i.e., the condition for which the energy content of the volatiles matches the total heat requirement of the process.

Exergy analysis

Pine was included here because the differences in gas and solid composition between pine and eucalyptus may lead to divergence in the exergy behavior. Chemical exergy of streams can be rather different even at similar energy efficiency ratios.

Results from exergy analysis are presented in Fig. 8 as a function of reactor temperature. Exergy yield exhibits a similar behavior for both species responding to the same criteria as for the energy yield. Biomass depolymerization during torrefaction occurs by different mechanisms; hence it generates organic acids and other carbon-containing compounds in a particular distribution for each biomass. Carbon content in the product is the limiting parameter for exergy, as demonstrated by Granados et al. (2014). Pine had higher exergy yields than eucalyptus

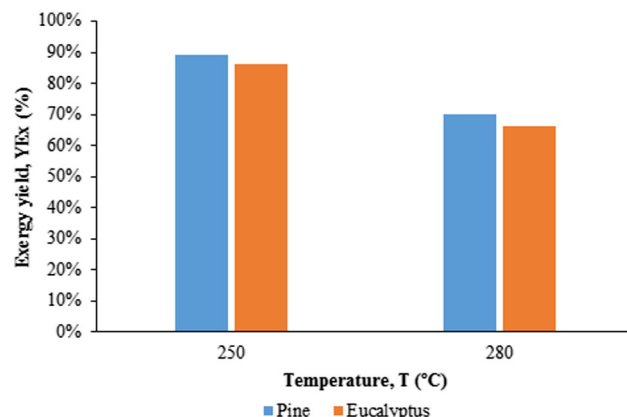


Fig. 8. Exergy yield and irreversibility in torrefaction of pine and Eucalyptus.

by 3–4%; however, irreversibility in torrefaction stage is higher for the former, leading to a higher exergy destruction ratio (22%).

From the point of view of process synthesis, it is recommended to burn volatiles in a post-combustion stage; otherwise, their exergy content should be considered as a waste, with the corresponding system efficiency penalty.

Evaluation of alternative 2

Alternative 2 in Fig. 2 was evaluated to determine the effect of feedstock pre-drying by taking advantage of torgas sensible heat. The exit temperature of torgas, after it is used for biomass drying, was fixed at 150 °C to maintain condensable components in the vapor fraction. The fraction of total drying heat supplied by torgas was estimated for both 250 and 280 °C, and the process was simulated considering the base case conditions (see Table 5). Moreover, we estimated the moisture amount at pre-drying stage exit uses the sensible heat previously mentioned.

It turns out that the sensible heat of torrefaction gases is not sufficient to satisfy the drying energy requirement; only a small fraction of this heat (<2.5%) can be supplied. Considering this, we concluded that pre-drying with torgas has a negligible effect on the overall thermal efficiency of the system and the extra wood required remains constant for both Alt. 1 and Alt. 2 in Fig. 2. Based on these results, the proposed process scheme (Alt.2) is a valid alternative to that reported by Kiel et al. (2012). The relative advantages require economic and environmental considerations and are the subject of our continuing studies.

Conclusions

A comprehensive torrefaction model using experimental data for two different wood species (*Eucalyptus globulus* and *Pinus radiata*) was developed. Best results were obtained for eucalyptus, which exhibited energy efficiencies between 81% and 96% depending on moisture content and torrefaction temperature. The volatiles can supply up to 90% of the heat consumed in the reactor, but autothermal operation was not reached under the conditions studied. It was demonstrated that hemicellulose structure influences the energy and exergy yields and exergy destruction ratios. With respect to the energy and exergy content of volatiles, best results are obtained for hardwoods (eucalyptus) with a high content of xylans. Exergy content of volatiles should be exploited in a post-combustion unit to reduce the losses. Exergy yield exhibited best results at 250 °C due to the retention of basic structures of woody biomass; operation at 280 °C produces more extensive depolymerization and more C-containing compounds in the volatiles. The absence of commercial torrefaction plants makes this modeling tool valuable for sustainability predictions. Integration with environmental analysis tools should lead to the development of this technology under sustainable conditions. Further studies to develop specific models for detailed reactor design giving priority to heat transfer and heat recovery systems are under way.

Acknowledgments

This work has been supported financially by the projects INNOVA CHILE 14IDL4-30438, FONDEF B09I1015 and Basal CONICYT PFB-27 of the Technological Development Unit of University of Concepción, Chile.

References

Agar D, Withersaari M. Bio-coal, torrefied lignocellulosic resources – key properties for its use in co-firing with fossil coal – their status. *Biomass Bioenergy* 2012;44:107–11.

Almeida G, Brito JO, Perré P. Alterations in energy properties of eucalyptus wood and bark subjected to torrefaction: the potential of mass loss as a synthetic indicator. *Bioresour Technol* 2010;101(24):9778–84.

Amos WA. Report on biomass drying technology report on biomass drying technology. [November] <http://www.nrel.gov/docs/fy99osti/25885.pdf>, 1998. [Available from].

Asimptote B v. Cycle tempo. [Internet] <http://www.asimptote.nl/software/cycle-tempo>, 2014. [Available from].

Basu P. Biomass gasification, pyrolysis and torrefaction. Practical design and theory. New York: Elsevier; 2013.

Bates RB, Ghoniem AF. Biomass torrefaction: modeling of volatile and solid product evolution kinetics. *Bioresour Technol* 2012;124:460–9.

Bates RB, Ghoniem AF. Biomass torrefaction: modeling of reaction thermochemistry. *Bioresour Technol* 2013;134:331–40.

Batidzirai B, Mignot PR, Schakel WB, Junginger HM, Faaij PC. Biomass torrefaction technology: techno-economic status and future prospects. *Energy* 2013;62:196–214.

Berg A, Díaz M, Bidart C, Pacheco A, Espinoza D, Praus S, et al. Estudio "Recomendaciones para la elaboración de una Estrategia Nacional de Bioenergía. Concepción: Ministerio de Energía; 2013 [Chile].

Bryden KM, Ragland KW, Rutland CJ. Modeling thermally thick pyrolysis of wood. *Biomass Bioenergy* 2002 Jan;22(1):41–53.

Burhenne L, Messmer J, Aicher T, Laborie M-P. The effect of the biomass components lignin, cellulose and hemicellulose on TGA and fixed bed pyrolysis. *J Anal Appl Pyrolysis* 2013;101:177–84.

Channiwala SA, Parikh PP. A unified correlation for estimating HHV of solid, liquid and gaseous fuels. *Fuel* 2002;81:1051–63.

Chen W-H, Kuo P-C. Torrefaction and co-torrefaction characterization of hemicellulose, cellulose and lignin as well as torrefaction of some basic constituents in biomass. *Energy* 2011;36(2):803–11.

Chen Z, Hu TQ, Jang HF, Grant E. Modification of xylan in alkaline treated bleached hardwood kraft pulps as classified by attenuated total-internal-reflection (ATR) FTIR spectroscopy. *Carbohydr Polym* 2015;127:418–26.

Chew JJ, Doshi V. Recent advances in biomass pretreatment – torrefaction fundamentals and technology. *Renew Sustain Energy Rev* 2011;15(8):4212–22.

D3172. Standard Practice for Proximate Analysis of Coal and Coke. ASTM; 2013 Available at: <http://www.astm.org/Standards/D3172.htm>

D5865–13 A. Standard Test Method for Gross Calorific Value of Coal and Coke. ASTM; 2013. Available at: <http://www.astm.org>

Di Blasi C, Lanzetta M. Intrinsic kinetics of isothermal xylan degradation in inert atmosphere. *J Anal Appl Pyrolysis* 1997;40 – 41:287–303.

Esteves Costa CA, Rodríguez Pinto PC, Rodríguez AE. Evaluation of chemical processing impact on E. globulus wood lignin and comparison with bark lignin. *Ind Crops Prod* 2014;61:479–91.

Felfli FF, Luengo CA, Soler PB. Mathematical modelling of wood and briquettes torrefaction. *A 5 Encontro Energia Meio Rural*. Brazil; 2004.

Fisher EM, Dupont C, Darvell LI, Commandré J-M, Saddawi JM. Combustion and gasification characteristics of chars from raw and torrefied biomass. *Bioresour Technol* 2012;119:157–65.

Gassner M, Maréchal F. Thermo-economic process model for thermochemical production of Synthetic Natural Gas (SNG) from lignocellulosic biomass. *Biomass Bioenergy* 2009;33(11):1587–604.

Granados D, Velásquez HI, Chejne F. Energetic and exergetic evaluation of residual biomass in a torrefaction process. *Energy* 2014;74:181–9.

Harouna IG, Sanogo O, Daho T, Ouimingua SK, Dan-Maza A, Nana B, et al. Determination of processes suitable for cotton stalk carbonization and torrefaction by partial combustion using a metal kiln. *Energy Sustain Dev* 2015;24:50–7.

Holmberg H, Ahtila P. Evaluation of energy efficiency in biofuel drying by means of energy and exergy analyses. *Appl Therm Eng* 2005;25(17–18):3115–28.

Joshi Y, de Vries H, Woudstra T, de Jong W. Torrefaction: unit operation modelling and process simulation. *Appl Therm Eng* 2014;2–7.

Kiel J, Zwart R, Verhoeff F. Torrefaction by ECN; 2012.

Kokko L, Tolvanen H, Hämäläinen K, Raiko R. Comparing the energy required for fine grinding torrefied and fast heat treated pine. *Biomass Bioenergy* 2012;42:219–23.

Koppejan J, Sokhansanj S, Staffan M, Sebem M. Status overview of torrefaction technologies. IEA Task 32. Enschede; 2012.

Kotas T. The exergy method of thermal plant analysis. Florida: KP; 1995.

Nag A. Biofuels refining and performance. 1st ed. San Francisco: McGraw-Hill Co.; 2008.

Nhuchhen D, Basu P, Acharya B. A comprehensive review on biomass torrefaction. *Int J Renew Energy Biofuels* 2014;1–56.

Park C, Zahid U, Lee S, Han C. Effect of process operating conditions in the biomass torrefaction: a simulation study using one-dimensional reactor and process model. *Energy* 2015;79:127–39.

Peduzzi E, Boissonnet G, Haarlemmer G, Dupont C, Maréchal F. Torrefaction modelling for lignocellulosic biomass conversion processes. *Energy* 2014;70:58–67.

Phanphanich M, Mani S. Impact of torrefaction on the grindability and fuel characteristics of forest biomass. *Bioresour Technol Elsevier* 2011 Jan;102(2):1246–53.

Pighinelli A, Boateng A, Mullen C, Elkasabi Y. Evaluation of Brazilian biomasses as feedstocks for fuel production via fast pyrolysis. *Energy Sustain Dev* 2014;21:42–50.

Prins MJ, Ptasiński KJ, Janssen FJJG. More efficient biomass gasification via torrefaction. *Energy* 2006a;31(15):3458–70.

Prins MJ, Ptasiński KJ, Janssen FJJG. Torrefaction of wood. *J Anal Appl Pyrolysis* 2006b;77(1):28–34.

Repellin V, Govin A, Rolland M, Guyonnet R. Modelling anhydrous weight loss of wood chips during torrefaction in a pilot kiln. *Biomass Bioenergy* 2010;34(5):602–9.

Reyes P, Teixeira R, Rodriguez J, Fardim P, Vega B. Characterization of the hemicellulosic fraction obtained after pre-hydrolysis of *Pinus radiata* wood chips with hot-water at different initial pH. *J Chil Chem Soc* 2013;58(1).

Rosillo-Calle F, de Groot P, Hemstock S. Biomass assessment handbook – bioenergy for a sustainable environment. 1st ed. London, UK: Routledge; 2010.

- Sarvaramini A, Assima GP, Larachi F. Dry torrefaction of biomass – torrefied products and torrefaction kinetics using the distributed activation energy model. *Chem Eng J* 2013; 229:498–507.
- Syu FS, Chiueh PT. Process simulation of rice straw torrefaction. *Sustain Environ Res* 2012; 22(3):177–83.
- Szargut J, Styrylska T. Approximate evaluation of the exergy of fuels. *Brennst Warne Kraft* 1964;16:589–96.
- Tumuluru J, Sokhansanj S, Wright CT, Boardman RD, Hess JR. Review on biomass torrefaction process and product properties and design of moving bed torrefaction system model development. Kentucky: The INL US Department of Energy; 2011.
- Uemura Y, Tsutsui T, Subbarao D, Yusuo S. Relationship between calorific value and elementary composition of torrefied lignocellulosic biomass. *J Appl Sci* 2010; 10(24):3250–6.
- Van der Stelt MJC, Gerhauser H, Kiel JH, Ptasinski KJ. Biomass upgrading by torrefaction for the production of biofuels: a review. *Biomass Bioenergy* 2011; 35(9):3748–62.
- Zakri B, Saari J, Sermyagina E, Vakkilainen E. Integration of torrefaction with steam power plant. Finland: Lappeenranta University 978-952-265-395-6; 2013 http://www.doria.fi/xmlui/bitstream/handle/10024/94111/Biotuli_torrefointi_tutkimusraportti.pdf?sequence=2 [Available at].